

Zbigniew Pędzich<sup>1\*</sup>, Robert Jasionowski<sup>2</sup>, Magdalena Ziąbka<sup>1</sup>

<sup>1</sup> AGH - University of Science and Technology, Faculty of Materials Science and Ceramics, Department of Ceramics and Refractory Materials  
al. A. Mickiewicza 30, 30-059 Krakow, Poland

<sup>2</sup> Maritime Academy, Institute of Basic Technical Sciences, Department of Shipbuilding Materials Engineering, ul. Podgórna 51-53, 70-506 Szczecin, Poland

\*Corresponding author. E-mail: pedzich@agh.edu.pl

Received (Otrzymano) 27.10.2013

## CAVITATION WEAR OF CERAMICS - PART I. MECHANISMS OF CAVITATION WEAR OF ALUMINA AND TETRAGONAL ZIRCONIA SINTERED POLYCRYSTALS

The usage of ceramic materials in applications endangered by intensive cavitation could limit erosion phenomena. In the presented work, cavitation erosion resistance of commonly used oxide phases ( $\alpha$ -alumina, tetragonal zirconia) in structural application were investigated. Volumetric wear of both materials was compared to the wear rate of FeAl48 alloy. Both oxides were more resistant for cavitation than intermetallic phase. Observations by means of SEM technique showed that surface destructions run in a similar way for both investigated oxides. The degradation proceeded by removing of the whole grains from sintered body. However, in the alumina grains were removed from a wide area, opposite to the zirconia material, which was degraded in limited, ribbon-like areas. In this case destruction reached deeper than only the one grain into material.

**Keywords:** cavitation, erosion, alumina, tetragonal zirconia

## ZUŻYCIE KAWITACYJNE CERAMIKI - CZĘŚĆ I. MECHANIZMY ZUŻYCIA KAWITACYJNEGO SPIEKÓW Z TLENKU GLINU I TETRAGONALNEGO DWUTLENKU CYRKONU

Użycie materiałów ceramicznych w zastosowaniach, w których materiał narażony jest na intensywne kawitację, może ograniczyć zużycie. W prezentowanej pracy zbadano odporność na zużycie kawitacyjne powszechnie stosowanych faz tlenkowych ( $\alpha$ -tlenku glinu i tetragonalnego dwutlenku cyrkonu). Zużycie objętościowe obu materiałów porównano ze zużyciem stopu FeAl48. Oba tlenki były odporniejsze na zużycie niż faza międzymetaliczna. Stwierdzono, że dwutlenek cyrkonu jest odporniejszy na erozję kawitacyjną. Obserwacje SEM pokazały, że destrukcja powierzchni przebiega w obu tlenkach w podobny sposób. Zniszczenie polega na usuwaniu całych ziaren ze spieków. Jednakże, ziarna tlenku glinu usuwane są jako monoziarnowa warstwa na stosunkowo dużej powierzchni, a ziarna dwutlenku cyrkonu usuwane są z obszarów wzdłuż nieregularnych linii na głębokość co najmniej kilku ziaren.

**Słowa kluczowe:** kawitacja, erozja, tlenek glinu, tetragonalny dwutlenek cyrkonu

### INTRODUCTION

Cavitation is a phenomenon caused by the repeated nucleation, growth, and violent collapse of clouds of bubbles within the liquid. Microstreams of liquid developed during the implosion of cavitation bubbles as well as the action of pressure waves from disappearing bubbles are the main causes of destruction on swilled surfaces leading to a loss of material, i.e. to cavitation erosion. On the surface of the material exposed to the acting of liquid, the cavitation phenomenon induces local destruction of the surface layer as a consequence of the resultant effect of liquid micro-stream blows with high hydrodynamic parameters as well as pressure waves. Due to the nature of loading, destruction of

material surface can be compared to the fatigue process [1-3]. This means that materials with larger resistance to cavitation erosion are first of all characterised by high hardness and micro-hardness as well as fine-grained one-phase microstructure having internal compressive stresses [4-6]. Among metallic materials the progress in cavitation resistance could be achieved by the application of intermetallic phases [7, 8]. Also ceramic materials could be perspective for such applications. The problem of devastation of fluid-flow machinery components is very complex. It consists of processes of erosion and corrosion. The use of ceramic materials in the applications endangered by intensive

cavitation could limit corrosion phenomena. The number of works devoted to the investigation of resistance to cavitation erosion of ceramics materials is not large [9-14] and they concern the properties of pure phases, such as alumina, zirconia silicon nitride or some glass types. As the result, the mentioned works gave some useful data suggesting which phases could be more resistant than the others and how the microstructure of sinters could influence the susceptibility to cavitation wear of ceramic phases.

In presented work, cavitation erosion resistance of commonly used oxide phases ( $\alpha$ -alumina, tetragonal zirconia) in structural application were investigated. Experimental results presented in the paper show properties of oxide phases often used as composite matrices. Next parts of work will present properties of composites basing on mentioned matrices.

## EXPERIMENTAL

Cavitation wear investigations were conducted for two types of ceramic sinters - the widely used oxide materials:  $\alpha$ -alumina and tetragonal zirconia. For the sinters fabrication commercial powders were applied:  $\text{Al}_2\text{O}_3$  - TM-DAR, produced by Taimicron Inc. (Japan), and yttria stabilized  $\text{ZrO}_2$  powder 3Y-TZ, Tosoh (Japan). The materials for investigations are marked in this work as follows: **A**, **Z**, for alumina, zirconia, respectively.

The sinters were fabricated in not a complicated way. Samples were uniaxially pressed under 50 MPa, consequently isostatically re-pressed under 300 MPa and then pressureless sintered at 1500 (for **A**) or 1550°C (for **Z**). The dwelling time of 2 hours was the same for all the mentioned samples.

The relative density of materials was calculated as a quotient of the apparent density and the theoretical one. The apparent density of materials was measured by Archimedian method. Theoretical density for alumina is  $3.99 \text{ g/cm}^3$ , and for applied zirconia material  $6.1 \text{ g/cm}^3$  (according producers data).

The hardness ( $HV$ ) and the fracture toughness ( $K_{Ic}$ ) were measured by Vickers indentation method, basing on Niihara calculation model [15], using Nanotech MV-700 equipment. The load was 49.05 N for hardness measurements and 98.1 N for  $K_{Ic}$  calculations. The data for strength analysis were collected from three-point bending tests made on  $30 \times 2.5 \times 2 \text{ mm}$  bars. The selected parameters of sinters are collected in Table 1.

The examination of cavitation erosion was carried out on a jet-impact device described in detail in [7]. The samples for the examination were of cylindrical shape, 20 mm in diameter and  $6 \pm 0.5 \text{ mm}$  height. Sample surface roughness, measured by means of PGM-1C profilometer, was about  $0.03 \mu\text{m}$ . The samples were mounted vertically in rotor arms, parallel to the axis of water stream pumped continuously at 0.06 MPa through a nozzle with a 10 mm diameter, 1.6 mm away from the

sample edge. The rotating samples stroke against the water stream. Water flow intensity was constant and amounted to  $1.55 \text{ m}^3/\text{h}$ . The wear rate was determined by sample weighing up to the total time of 2400 minutes. Volumetric wear rate was calculated as a quotient of weight loss and apparent density of each investigated sample. Calculations were performed after 500, 900, 1200, 1500, 1800 and 2400 minutes of test duration.

TABLE 1. Selected properties of investigated ceramic sinters  
TABELA 1. Wybrane właściwości niektórych spieków ceramicznych

Material	Apparent density [g/cm <sup>3</sup> ]	Relative density [% of theo.]	Vicker's hardness $HV_5$ [GPa]	Young modulus $E$ [GPa]	Fracture toughness $K_{Ic}$ [MPa <sup>m<sup>0.5</sup>]</sup>	Bending strength $\sigma$ [MPa]
$\text{Al}_2\text{O}_3$	$3.96 \pm 0.1$	99.3	$17.0 \pm 1.2$	$379 \pm 6$	$3.6 \pm 0.3$	$600 \pm 120$
$\text{ZrO}_2$	$6.07 \pm 0.1$	99.5	$14.0 \pm 0.5$	$209 \pm 5$	$5.0 \pm 0.5$	$1150 \pm 55$

Worn materials surfaces were observed by means of SEM technique with FEI NOVA NANO 200 device.

## RESULTS

The basic results of the test are collected in Figure 1. It presents the volumetric wear of investigated ceramic materials during the stream impact test compared to the wear of the iron aluminide FeAl48. This intermetallic alloy was regarded to be the one of less susceptible to cavitation wear [7].

As it could be recognized, ceramic phases were resistant to cavitation wear, yet the difference between alumina and zirconia was distinct.

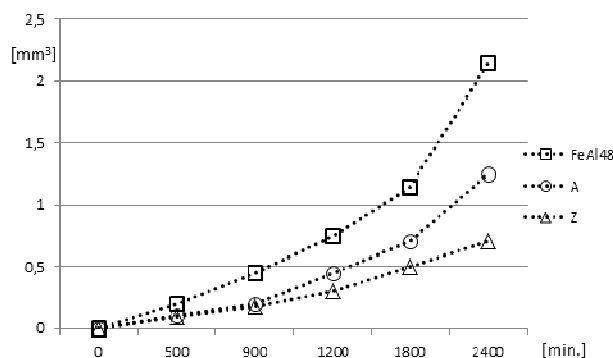


Fig. 1. Volumetric wear of investigated materials during the stream impact test

Rys. 1. Zużycie objętościowe materiałów badanych podczas testu strumieniowo-uderzeniowego

Figures 2-5 illustrate the state of the alumina sinter surface after the cavitation test, observed by means of SEM technique.

The firsts traces of wear appeared on alumina surface as isolated holes left behind removed single alumina grains (Fig. 2). During the test, the degradation proceeded and the next single grains were removed. Figures 3a and 3b present a general view of the degra-

dation progress. The detail observation of destroyed areas revealed that the alumina surface was damaged by removing of single layer of whole grains (Fig. 4). The cases of transgranular cracking were very rare as it could be visible in the Figure 5.

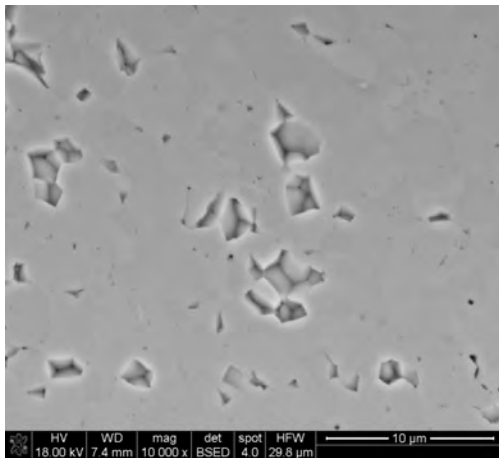


Fig. 2. Typical SEM image of the first traces of alumina surface degradation

Rys. 2. Typowy obraz SEM pierwszych śladów degradacji powierzchni tlenku glinu

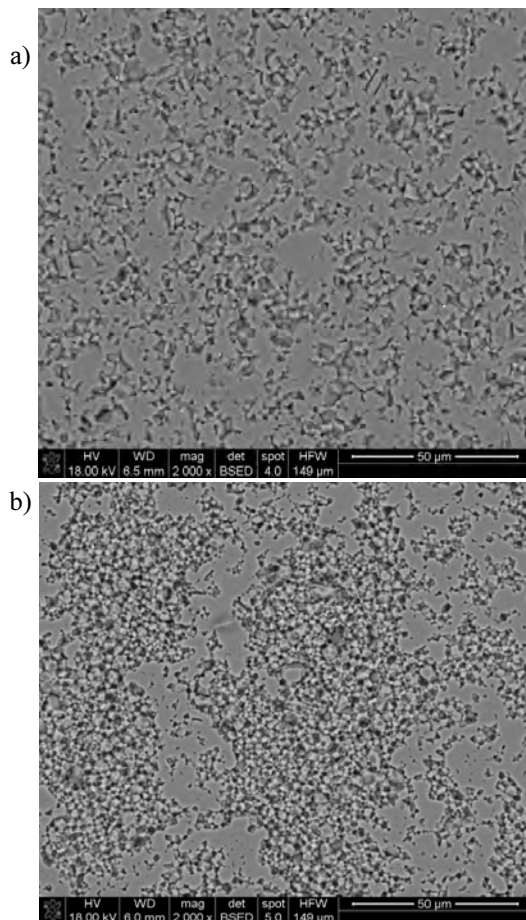


Fig. 3. SEM micrographs illustrating erosion progress on the alumina surface: a) typical wear traces after 900 min, b) typical wear traces after 1200 min.

Rys. 3. Mikrofotografie SEM ilustrujące postęp zużycia powierzchni tlenku glinu: a) typowe ślady zużycia po 900 min, b) typowe ślady zużycia po 1200 min

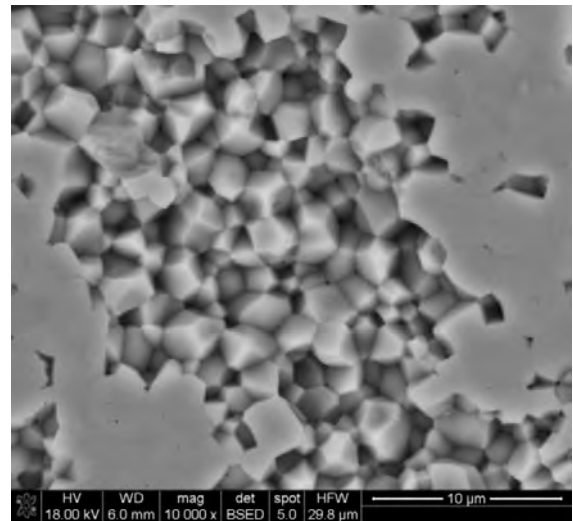


Fig. 4. SEM micrograph illustrating erosion of alumina in a monolayer mode

Rys. 4. Mikrofotografia SEM ilustrująca monowarstwową erozję tlenku glinu

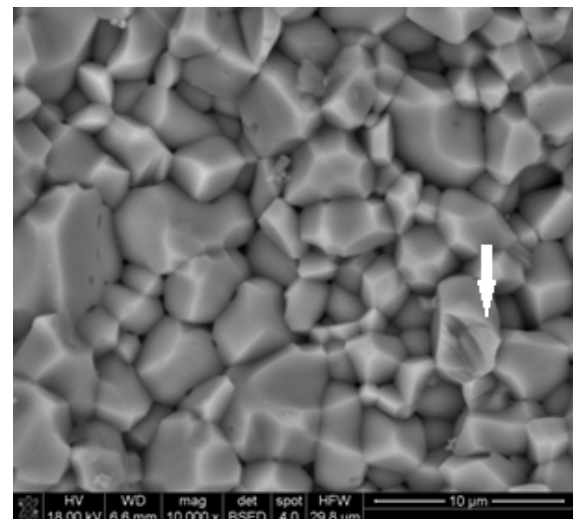


Fig. 5. SEM micrograph illustrating erosion of alumina by removing in general the whole grains. The case of transgranular cracking was marked with a white arrow

Rys. 5. Mikrofotografia SEM ilustrująca erozję tlenku glinu głównie poprzez usuwanie całych ziaren. Przypadek pęknięcia wzdłuż ziarnowego zaznaczono białą strzałką

Figures 6 and 7 illustrate zirconia surfaces after the cavitation test. Observations of SEM micrographs confirmed the results of volumetric loss of materials measurements. The images showed also differences in destruction mechanisms for the investigated materials. Comparison of both oxides **A** and **Z** showed that surface destruction run in a similar way. It means that degradation proceeded by removing the whole grains from the sintered body. However, in alumina the grains were removed from a wide area, opposite to the zirconia material, which was degraded in limited, ribbon-like areas. In this case destruction reached deeper than one grain into the material. It is clearly visible in Figure 7. Such a difference in the degradation mechanisms resulted in a distinct difference in volumetric wear. The

investigated zirconia sinter was much more resistant to cavitation than the alumina one.

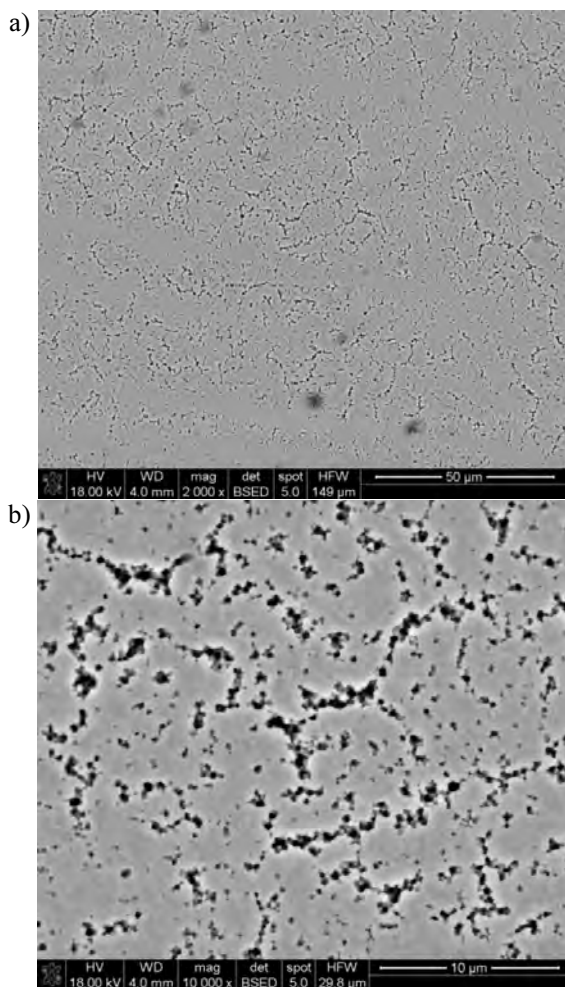


Fig. 6. Typical SEM images of zirconia sample surface after the cavitation test - 2400 min: a), b) different magnifications of the same area

Rys. 6. Typowe obrazy SEM powierzchni dwutlenku cyrkonu po teście kawitacyjnym - 2400 min: a), b) różne powiększenia tego samego obszaru

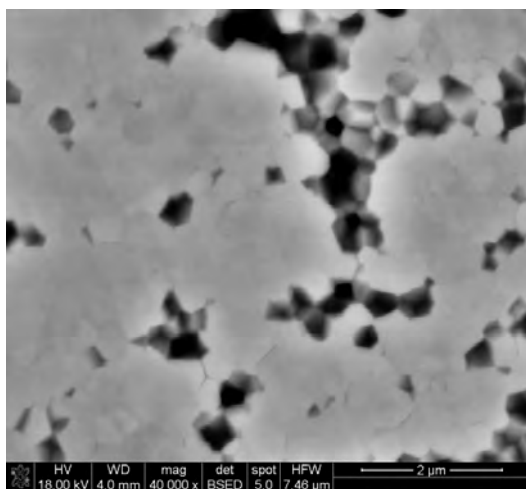


Fig. 7. The SEM image of zirconia sample surface erosion illustrating the depth of worn area

Rys. 7. Obraz SEM erozji powierzchni próbki dwutlenku cyrkonu ilustrujący głębokość zużytej strefy

Differences in the degradation mechanisms for both investigated oxide phases were probably caused by two factors. The first one was generally a large difference in the mean grain size in the investigated sinters. This parameter was not precisely determined during investigations but the estimation made on micrographs indicated that there was about a one order of magnitude difference between the mean grain size in alumina (~ a few micrometers) and the mean grain size in zirconia (~ hundreds of nanometers). During the cavitation test the pressure caused microcracking along grain boundaries. Propagation of these cracks was easier in the material with the lower grain boundary density (alumina).

The second reason of the difference in the cavitation wear behaviour between alumina and zirconia was most probably tetragonal to the monoclinic phase transformation which took place when microcracks appeared near the tetragonal zirconia grains. This was the reason why damage in zirconia polycrystals went into the depth of the material.

## SUMMARY

The performed cavitation wear tests by the stream-impact method revealed differences in wear mechanisms for alumina and tetragonal zirconia phases. In both materials degradation runs by removal of whole grains. The volumetric wear of zirconia was much lower than this measured for alumina.

In alumina the progress of this process is spread in a mono-grain layer on a relatively large surface. In zirconia the grain removal process runs along ribbon-like paths in the volume larger than one grain.

## Acknowledgements

*The research has been funded by the Ministry of Education and Science as the AGH - University project no. 11.11.160.603-1.*

## REFERENCES

- [1] Brennen C.E., Cavitation and Bubble Dynamics, Oxford University Press, 1995.
- [2] Briggs L.J., The limiting negative pressure of water, Journal of Applied Physics 1970, 21, 721-722.
- [3] Trevena D.H., Cavitation and Tension in Liquids, IOP Publishing Ltd., 1987.
- [4] Plesset M.S., Chapman R.B., Collapse of an initially spherical vapour cavity in the neighbourhood of a solid boundary, Jour. Fluid Mech. 1971, 47(2), 283-290.
- [5] Hickling R., Plesset M.S., Collapse and rebound of a spherical bubble in water, Phys. Fluids 1963, (7), 7-14.
- [6] Naude C.F., Ellis A.T., On the mechanism of cavitation damage by non-hemispherical cavities collapsing in contact with a solid boundary, Journal of Basic Engineering 1961, 83, 648-656.
- [7] Jasionowski R., Przetakiewicz W., Zasada D., The effect of structure on the cavitation wear of FeAl intermetallic

- phase-based alloys with cubic lattice, *Archives of Foundry Engineering*, 2011, 11, Special Issue 2, 97-102.
- [8] Schneibel J.H., George E.P. Anderson I.M., Tensile ductility, slow crack growth and fracture mode of ternary B2 iron aluminides at room temperature, *Intermetallics* 1997, 5, 185-193.
- [9] Tomlinson W.J., Matthews S.J., Cavitation erosion of structural ceramics, *Ceramics International* 1994, 20(3), 201-209.
- [10] Tomlinson W.J., Kalitsounakis N., Vekinis G., Cavitation erosion of aluminas, *Ceramics International* 1999, 25(4), 331-338.
- [11] Niebuhr D., Cavitation erosion behavior of ceramics in aqueous solutions, *Wear* 2007, 263(1-6), 295-300.
- [12] Garcia-Atance Fatjo G., Hadfield M., Tabeshfar K., Pseudoplastic deformation pits on polished ceramics due to cavitation erosion, *Ceramics International* 2011, 37, 1919-1927.
- [13] Lua J., Zum Gahr K.-H., Schneider J., Microstructural effects on the resistance to cavitation erosion of ZrO<sub>2</sub> ceramics in water, *Wear* 2008, 265, 1680-1686.
- [14] Pędzich Z., Jasionowski R., Lach R., Przetakiewicz W., Cavitation Resistance of Sintered Alumina and Composites on Its Base, [In:] *Innovative Manufacturing Technology 2*, Ed. P. Rusek, Institute of Advanced Manufacturing Technology, Krakow 2012, 393-402.
- [15] Niihara K., A fracture mechanics analysis of indentation, *J. Mater. Sci. Lett.* 1983, 2, 221-223.